RSC Advances

PAPER

View Article Online
View Journal | View Issue

Published on 01 November 2016. Downloaded by University of Newcastle on 07/01/2017 02:00:00.

Cite this: *RSC Adv.*, 2016, **6**, 105638

Immobilizing AgPd alloy on Vulcan XC-72 carbon: a novel catalyst for highly efficient hydrogen generation from formaldehyde aqueous solution†

Shutao Gao, Tao Feng, Qiuhua Wu, Cheng Feng,* Ningzhao Shang and Chun Wang*

Received 12th September 2016
Accepted 30th October 2016

DOI: 10.1039/c6ra22761a

www.rsc.org/advances

A novel bimetallic catalyst, AgPd nanoalloy supported on Vulcan XC-72 carbon (AgPd@C-72), has been successfully fabricated and used for catalyzing H_2 generation from formaldehyde aqueous solution at room temperature for the first time. The catalyst exhibits high catalytic activity and good stability, and the hydrogen generation rates could reach up to 237.4 mL min^{-1} g^{-1}, which could be attributed to the high dispersion of metal nanoparticles, the synergistic effect of bimetal AgPd, and distinct interaction between the bimetal and the support. The excellent performance of the new catalytic system renders it quite attractive as a superior competitor for efficient hydrogen production from formaldehyde at room temperature. This work might open up a new way to further develop cost-effective and highly efficient bimetallic catalysts for the generation of H_2 from formaldehyde aqueous solution.

Introduction

Owing to industrial development and population growth, the world's energy consumption is dramatically increasing. This increasing energy demand makes it necessary to develop more secure and diversified energy sources because the present world energy supply comes mainly from fossil fuels that are rapidly depleting.[1] Among the various alternative energy strategies, hydrogen is one of the most promising candidates to replace nonrenewable fuel sources and is foreseen to become a major energy carrier in the relatively close future because it is a renewable, environmentally friendly energy carrier.[2,3] However, searching for safe and efficient hydrogen storage materials remains one of the most difficult challenges for the transformation from the present fossil fuel economy to a hydrogen economy.[4–7] In this context, one of the promising hydrogen storage techniques relies on liquid-phase chemical hydrogen storage materials.[2]

Up to now, various liquid-phase chemical hydrogen storage materials such as aqueous sodium borohydride,[8–10] ammonia borane,[11–13] hydrazine,[14,15] formic acid,[5,16–19] and formaldehyde,[20–22] have been intensively studied by various research groups. Among them, hydrogen generation from formaldehyde is of significant importance since it can combine hydrogen generation with destruction of formaldehyde, an environmental pollutant, together. Usually, this reaction occurs in an alkaline solutions and the efficiency of hydrogen generation is very low. To accelerate the rate of hydrogen production from formaldehyde solution, adding catalyst into the alkaline formaldehyde solutions is necessary. Several reports have confirmed that nanometallic catalysts, such as Cu, Au, Pt, Ni, and Ag, can significantly accelerate the hydrogen production rate at atmospheric pressure.[23–27] However, using metal nanoparticles as catalysts suffers from a serious intrinsic defect: metal nanoparticles inevitably tend to agglomerate into large particles, which greatly decrease the active site, thus reduce the catalytic performances. Therefore, it is highly desirable to develop an effective strategy to prevent metal nanoparticles from agglomeration and improve the catalytic performance of the catalysts.

In this regards, immobilizing metal nanoparticles on suitable supports to obtain well-dispersed metal nanoparticles is a very effective and the most common method to prevent agglomeration of metal nanoparticles and improve the activity and stability of catalysts. It has been demonstrated that the synergetic interaction between the metal and support, the type of the support, and the dispersity of the metal nanoparticles play an important role in the catalytic performance of the nanocatalysts.[28,29] Carbon material is the most commonly used catalyst support material because of its large surface area, high electrical conductivity, and good thermal, chemical and mechanical stability. Up to now, various carbon material such as active carbon,[30] carbon nanotubes[31] and graphene[32] have been used as catalyst support material. As a commercially available and relatively cheap carbon material, Vulcan XC-72 has a good electrical and thermal conductivity and is considered as promising catalyst support material for the design of uniformly dispersed metal nanoparticles.[7,33–37]

College of Sciences, Agricultural University of Hebei, Baoding 071001, P. R. China . E-mail: chunwang69@126.com; fengchengcctv@163.com; Tel: +86 312 7528291

† Electronic supplementary information (ESI) available: The energy-dispersive X-ray spectroscopy and N_2 adsorption–desorption isotherms of the catalyst, hydrogen generation with different content of the catalyst, powder X-ray diffraction patterns of Ag_1Pd_4@C-72 and used catalyst, GC spectrum of the evolved H_2, ICP-AES results of AgPd@C-72 catalysts. See DOI: 10.1039/c6ra22761a

This journal is © The Royal Society of Chemistry 2016

Published on 01 November 2016. Downloaded by University of Newcastle on 07/01/2017 02:00:00.

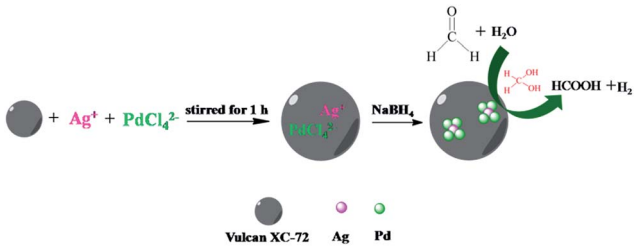

Scheme 1 Schematic representation of the synthesis process Ag_1Pd_4@C-72 and the hydrogen generation from formaldehyde aqueous solution.

Recently, bimetallic nanoparticles, a class of materials with a combination of properties that are associated with the two constituent metals, have emerged as an important class of catalysts. In many cases, bimetallic nanoparticles have higher catalytic efficiencies than their monometallic counterparts, owing to strong synergy between the metals. The addition of a second metal is an important approach for tailoring the electronic and geometric structures of nanoparticles to enhance their catalytic activity and selectivity.[38,39] Bimetallic catalysts have shown excellent catalytic properties for different chemical transformations including hydrogen generation reaction. For example, Pd–Au and Pd–Ag alloys supported on carbon materials have been developed for the catalytic dehydrogenation of formic acid, and the result indicated that the bimetallic catalysts, Pd–Au/C and Pd–Ag/C, showed a higher catalytic activity than their monometallic counterparts.[40,41] The addition of other metals could electronically promote Pd sites to significantly higher catalytic activity, as well as to a better tolerance toward CO poisoning *via* the synergetic effects between other metals and Pd.[36]

Keeping all above in mind, herein, a novel bimetallic catalyst, well dispersed AgPd alloy nanoparticles supported on Vulcan XC-72 carbon (AgPd@C-72), was fabricated *via* an *in situ* co-reduction method under mild conditions, and it was used as a catalyst for catalytic dehydrogenation of formaldehyde (Scheme 1). The AgPd@C-72 catalyst exhibited much higher catalytic activity, excellent stability and 100% H_2 selectivity for hydrogen generation from formaldehyde solution at room temperature. To the best of our knowledge, this is the first report on Vulcan XC-72 carbon-supported AgPd bimetallic catalyst for catalytic dehydrogenation of formaldehyde solution at room temperature.

Experimental

Chemicals and characterizations

Palladium(II) chloride ($PdCl_2$), 40% formaldehyde aqueous solution, sodium borohydride ($NaBH_4$, 96%) were purchased from Aladdin Reagent Limited Company (China). Silver nitrate ($AgNO_3$) and hydrochloric acid (HCl, 37%) were all obtained from Boaixin Chemical Reagents Company (Baoding, China) and used as received. Vulcan XC-72 carbon (Cabot Corp., USA) was used as received.

Transmission electron microscopy (TEM) studies were conducted on a JEOL model JEM-2011(HR) instrument. X-ray photoelectron spectroscopy (XPS) was performed with a PHI 1600 spectroscope. The X-ray diffraction (XRD) patterns of the samples were recorded with a TD-3700 X-ray diffractometer (China). The metal content of the materials was analyzed by a T.J.A. ICP-9000 type inductively coupled plasma atomic emission spectroscopy (ICP-AES) instrument. The surface area of the samples were measured at 77 K by nitrogen adsorption using a V-Sorb 2800P volumetric adsorption equipment (Jinaipu, China). The analysis of H_2 was performed on SP-2000 (China) with thermal conductivity detector (TCD).

Synthesis of AgPd@C-72 catalysts

For preparation of Ag_1Pd_4@C-72, 100 mg of Vulcan XC-72 carbon was dispersed in 50 mL water, then 1.65 mL 6.0 mmol L^{-1} silver nitrate and 6.6 mL 6.0 mmol L^{-1} H_2PdCl_4 solution was added, the mixture was stirred for 1 h at room temperature. Then 15 mg $NaBH_4$ was added into the above solution, the mixture was stirred for 3 h at room temperature to yield Ag_1Pd_4@C-72. After centrifugation and washing with water, the obtained Ag_1Pd_4@C-72 (the mass content of total metals was 5% and molar ratio of Ag and Pd was 1 : 4) was dried at 80 °C in vacuum overnight.

Ag_1Pd_1@C-72, Ag@C-72 and Pd@C-72 catalysts (the mass content of total metals was 5%) were synthesized with the above procedure except that the molar ratios of Ag and Pd were 1 : 1, 1 : 0 and 0 : 1, respectively. The contents of Ag and Pd in the composite were determined by ICP-AES as shown in Table S1 (see ESI†).

Activity tests

The as-prepared catalyst (15 mg) was added into the HCHO and NaOH aqueous solution (100 mL) to form a mixed solution, which was placed in a sealed 600 mL flask. Then the solution was placed in a water bath at a preset temperature under ambient atmosphere and stirred vigorously during the reaction. The volume of hydrogen gas evolved was measured by a gas chromatograph system equipped with TCD, which used argon as carrier gas. The amounts of the hydrogen produced were measured every five minutes, no carbon monoxide or other gaseous product can be detected in all these catalytic processes.

Results and discussion

The morphology of the as-prepared Ag_1Pd_4@C-72 composite is characterized by TEM. It can be seen that the AgPd nanoparticles supported on Vulcan XC-72 are well dispersed with an average particle size of about 3–6 nm (Fig. 1a), suggesting that Vulcan XC-72 leads to the good dispersion of metal nanoparticles on its surface. The corresponding energy-dispersive X-ray (EDX) spectrum (Fig. S1†) proves the existence of the Ag, Pd elements. Fig. 1b shows the high-resolution TEM (HRTEM) image of the as-prepared catalyst, wherein the lattice spacing is 0.23 nm, which is between the (111) lattice spacing of face-centered cubic (fcc) Ag (0.24 nm) and fcc Pd (0.22 nm), suggesting that Ag–Pd is formed as an alloy structure.

The crystallographic structure of the as-prepared AgPd@C-72 sample was examined by powder X-ray diffraction (PXRD).

Published on 01 November 2016. Downloaded by University of Newcastle on 07/01/2017 02:00:00.

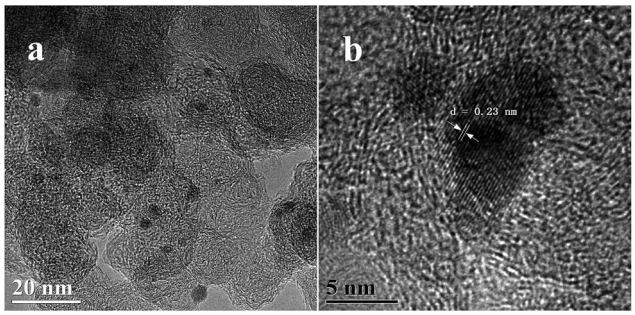

Fig. 1 TEM images (a and b) of Ag_1Pd_4@C-72.

Fig. 2 showed the PXRD patterns of Ag@C-72, Ag_1Pd_4@C-72 and Pd@C-72. It can be seen that all the as-prepared samples possess similar XRD patterns at $2\theta = 25.19°$, which is assigned to the Vulcan XC-72. Furthermore, the PXRD pattern of Ag_1Pd_4@C-72 exhibited a smaller peak between the characteristic peaks of Ag(111) ($2\theta = 38.42°$) and Pd(111) ($2\theta = 40.01°$), indicating the formation of the AgPd alloy, and also suggesting that the well dispersion of AgPd alloy NPs. Fig. S2† shows the PXRD patterns of the recycled Ag_1Pd_4@C-72 after four runs. It can be seen that there is no obvious change compared with that of the fresh prepared catalyst.

XPS analysis further confirms the presence of Ag, Pd and C in the Ag_1Pd_4@C-72 hybrid composites (Fig. 3). As shown in Fig. 3b and c, the $3d^{5/2}$ and $3d^{3/2}$ peak of Pd^0 appear at 335.9 eV and 341.2 eV, the $3d^{5/2}$ and $3d^{3/2}$ peak of Ag^0 appear at 368.3 eV and 374.2 eV. The results indicated that the co-existence of both metals. In addition, the presence of PdO species in Ag_1Pd_4@C-72 was confirmed by fitted the high energy shoulder on the metallic Pd lines at bond energy of about 338.2 and 343.1 eV. The production of oxidized Pd species could be due to the oxidation of metallic Pd left in an oxygen-containing environment.

The N_2 adsorption–desorption isotherms of Ag_1Pd_4@C-72 and Vulcan XC-72 are shown in Fig. S3.† The BET surface areas of Ag_1Pd_4@C-72 is 169.8 $m^2\ g^{-1}$, which is lower than Vulcan XC-72 (242.9 $m^2\ g^{-1}$). The results indicated that the external surface of Vulcan XC-72 is occupied by AgPd nanoparticles.

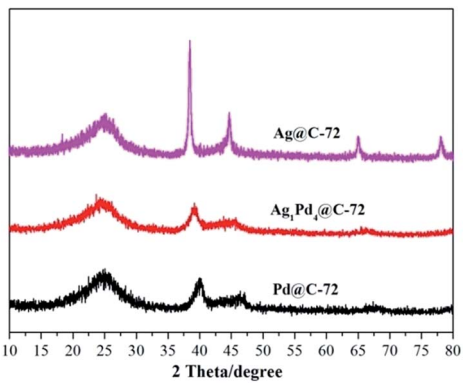

Fig. 2 Powder X-ray diffraction patterns of Pd@C-72, Ag_1Pd_4@C-72 and Ag@C-72.

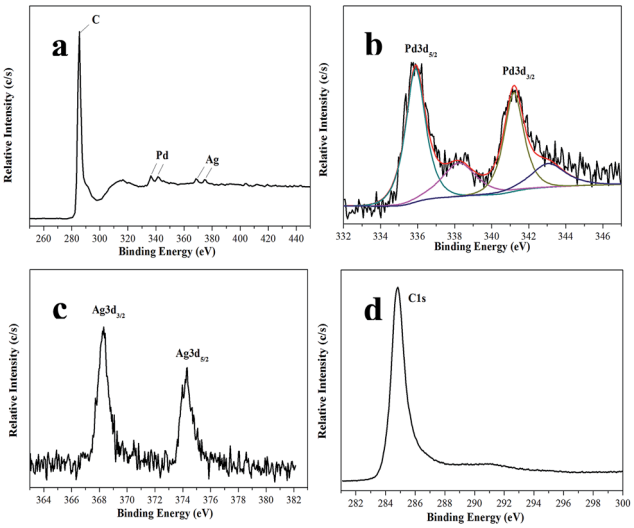

Fig. 3 XPS patterns of Ag_1Pd_4@C-72.

In order to enhance the H_2 generation rate and select optimal catalyst, the catalytic activity of different catalysts for the hydrogen production reaction from alkaline formaldehyde solution at 30 °C has been investigated based on the amount of gases generated volumetrically during the reaction. The results shown in Fig. 4 indicated that the catalytic activities were strongly depended on the composition of the catalysts. Remarkably, the bi-metallic AgPd@C-72 are more active than their monometallic counterparts, Ag@C-72 or Pd@C-72, which proving the synergistic effect of bimetallic AgPd alloy catalyst. Additionally, the mass ratio of Ag : Pd in the AgPd@C-72 system also play a crucial role in the catalytic activity, and Ag_1Pd_4@C-72 is found to be the most active one for formaldehyde dehydrogenation with a high rates of 237.4 mL $min^{-1}\ g^{-1}$. Moreover, as shown in Fig. S4,† the Ag_1Pd_4@C-72 catalyst with different content of metal can be found to exhibit different catalytic performance. The high activity of 5 wt% Ag_1Pd_4@C-72 could be attributed to the synergic effect between Vulcan XC-72 and AgPd bimetallic alloy, including the high specific surface areas of Vulcan XC-72, the well dispersion of

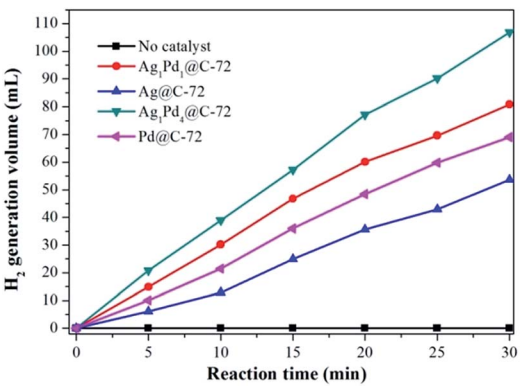

Fig. 4 Hydrogen generation by decomposition of HCHO with different ratios of AgPd supported on Vulcan XC-72 *versus* time at 30 °C, NaOH: 1.0 mol L^{-1}, HCHO: 0.26 mol L^{-1}, catalyst: 15 mg.

This journal is © The Royal Society of Chemistry 2016

Published on 01 November 2016. Downloaded by University of Newcastle on 07/01/2017 02:00:00.

AgPd nanoparticles on Vulcan XC-72. Hence 5 wt% Ag_1Pd_4@C-72 is selected as the optimum catalyst for catalyzing the dehydrogenation of formaldehyde.

In addition, the exclusive formation of H_2 has been confirmed by gas chromatography (GC) analyses (Fig. S5†) *via* comparing with pure H_2, indicating the excellent H_2 selectivity for formaldehyde dehydrogenation catalyzed by Ag_1Pd_4@C-72.

The effect of NaOH concentrations on the H_2 generation was also investigated. As shown in Fig. 5, the H_2 generation rate over Ag_1Pd_4@C-72 catalyst depends largely on the concentrations of NaOH. No H_2 gas evolution has been detected in the absence of NaOH, while H_2 generation reaction occurred immediately when a small amount of NaOH was added into the reaction system, indicating that the alkaline condition is indispensable for this catalytic process. When the NaOH concentrations were increased from 0.5 to 1.0 mol L^{-1}, the average rate of hydrogen production obviously increased. However, further increasing the NaOH concentration up to 3.0 and 5.0 mol L^{-1}, the rates of H_2 production decreased obviously, which may be due to the competition with the Cannizzaro reaction for transforming formaldehyde into the corresponding methanol and formic acid under highly alkaline conditions.[26,27]

The effect of HCHO concentration on H_2 generation has also been studied and the result was shown in Fig. 6. It can be clearly seen that H_2 generation rate was slow when the HCHO concentration was very low, and the highest rate of H_2 generation was obtained at 0.26 mol L^{-1}, but further increasing the concentration of formaldehyde up to 0.65 mol L^{-1} results in a decrease of H_2 generation rate, which suggest that high HCHO concentrations is disadvantageous for the H_2 generation reaction. The results indicate that the HCHO concentration plays a important role in determining the H_2 generation rate, and it is necessary to control appropriate HCHO concentration to achieve high H_2 generation rates.

The effect of reaction temperature on the rate of H_2 generation was investigated in the range of 15–30 °C, and the result was shown in Fig. 7. It can be clearly seen that the average H_2 generation rate increased rapidly from 102.5 to 237.4 mL min^{-1} g^{-1} when the temperature increased from 15 to 30 °C, which indicated that the high temperature is beneficial to

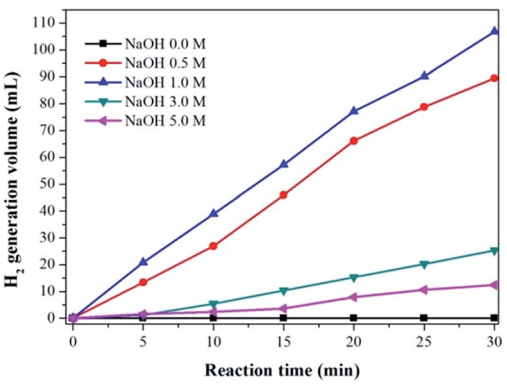

Fig. 5 Volume of the generated hydrogen by decomposition of HCHO with different concentration of NaOH, Ag_1Pd_4@C-72 catalyst: 15 mg, HCHO: 0.26 mol L^{-1}, temperature: 30 °C.

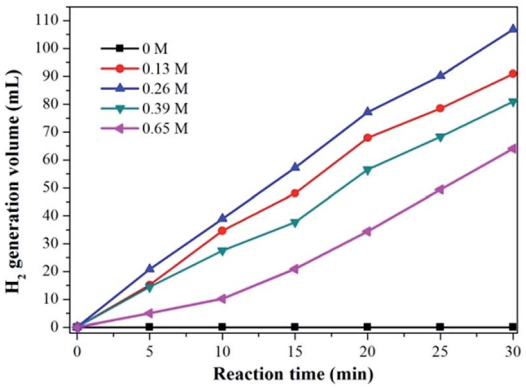

Fig. 6 Volume of the generated hydrogen with different concentration of HCHO, Ag_1Pd_4@C-72 catalyst: 15 mg, NaOH: 1.0 mol L^{-1}, temperature: 30 °C.

facilitating the H_2 generation reaction. Moreover, as shown in Fig. 7a, the amount of H_2 generated is linearly dependent on the reaction time at each temperature, suggesting that the H_2 generation reaction is a zero order reaction. Therefore, the reaction rate equation can be expressed as eqn (1):

$$K = A \exp(-E/RT) \quad (1)$$

where K is the rate constant, A is the frequency factor, E is the activation energy, R is the gas constant, and T is the absolute temperature. The activation energy E can be determined from the slope of the plot obtained by plotting ln K *versus* $1/T$. It is well known that the activation energy E plays a key role in determining the rate of a chemical reaction. The lower the activation energy, the faster the rate. Using the experimental data shown in Fig. 7a, the calculated activation energy E for the H_2 generation reaction with the catalyst was 39.16 kJ mol^{-1} (Fig. 7b), which was much lower than that of no catalyst participation, 65 kJ mol^{-1}.[42] The result demonstrated that the prepared Ag_1Pd_4@C-72 could serve as a highly efficient catalyst for catalyzing H_2 production from formaldehyde solution at room temperature.

The stability and reusability of catalyst is crucial for its practical application, so the reusability of the prepared Ag_1Pd_4@C-72 catalyst in the catalyzing dehydrogenation of formaldehyde was tested. As shown in Fig. 8, the catalytic

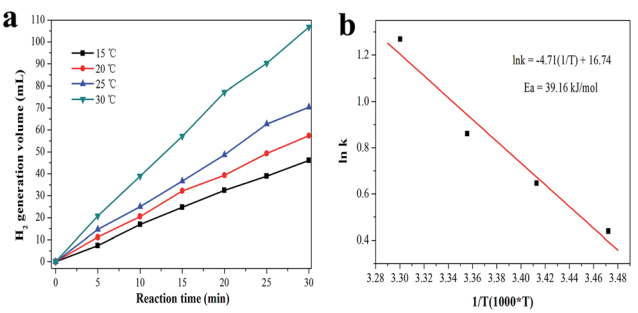

Fig. 7 The effect of reaction temperature on H_2 production (a), Ag_1Pd_4@C-72 catalyst: 15 mg, HCHO: 0.26 mol L^{-1}, NaOH: 1.0 mol L^{-1}; (b) the calculation of activation energy for Ag_1Pd_4@C-72.

Published on 01 November 2016. Downloaded by University of Newcastle on 07/01/2017 02:00:00.

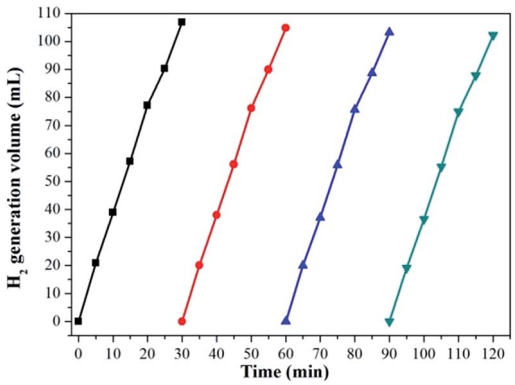

Fig. 8 Stability test on the Ag_1Pd_4@C-72 catalyst in the dehydrogenation of 0.26 M HCHO aqueous solution at 30 °C.

activity of Ag_1Pd_4@C-72 catalyst has no obvious decline after four runs, suggesting that the catalyst has a quite good stability, which should attribute to the fact that loading AgPd nanoparticles on the carbon matrix could efficiently prevent the agglomeration of metal nanoparticles. Thereby, Ag_1Pd_4@C-72 could efficiently catalyze formaldehyde to produce H_2 with an excellent catalytic activity and stability in alkaline aqueous solutions.

A possible mechanism for the high catalytic activity of the Ag_1Pd_4@C-72 is proposed. Firstly, formaldehyde is hydrated to form methylene glycol in the presence of NaOH, then the methylene glycol is transformed to hydrogen and sodium formate catalyzed by Ag_1Pd_4@C-72.[25] We think that the high catalytic activity of the Ag_1Pd_4@C-72 may be attributed to the AgPd nanoalloy structure, strong electron-donating effects of Vulcan XC-72 carbon on Pd, and the high adsorption ability of XC-72 carbon for formaldehyde.[36]

Conclusions

In this work, a novel bimetallic catalyst, the AgPd nanoalloy supported on Vulcan XC-72 carbon, has been successfully fabricated and applied as a stable and low-cost catalyst for H_2 generation from formaldehyde aqueous solution at room temperature. The results show that the Ag_1Pd_4@C-72 catalyst exhibit high catalytic activity and good stability. The hydrogen generation rates could reach up to 237.4 mL min^{-1} g^{-1}, which could attribute to the synergistic effect of bimetal AgPd, distinct interaction between bimetal and support, and high dispersion of metal nanoparticles. The excellent performance of the new catalyst renders it quite attractive as a superior competitor for efficient hydrogen production from formaldehyde. This work might open up a new way to further develop cost-effective and highly efficient bimetallic catalysts for the generation of H_2 from formaldehyde aqueous solution to meet the requirement of practical application of formaldehyde as a H_2 storage/generation material.

Acknowledgements

Financial supports from the National Natural Science Foundation of China (31671930, 21603054), the Natural Science Foundation of Hebei Province (B2015204003, B2016204131), the Young Top-notch Talents Foundation of Hebei Provincial Universities (BJ2016027), the Natural Science Foundation of Agricultural University of Hebei (LG201404, ZD201506, ZD201613), are gratefully acknowledged.

Notes and references

1 H. L. Jiang, S. K. Singh, J. M. Yan, X. B. Zhang and Q. Xu, *ChemSusChem*, 2010, **3**, 541–549.
2 M. Yadav and Q. Xu, *Energy Environ. Sci.*, 2012, **5**, 9698–9725.
3 Y. Ping, J.-M. Yan, Z.-L. Wang, H.-L. Wang and Q. Jiang, *J. Mater. Chem. A*, 2013, **1**, 12188–12191.
4 H. Dai, B. Xia, L. Wen, C. Du, J. Su, W. Luo and G. Cheng, *Appl. Catal., B*, 2015, **165**, 57–62.
5 Z.-L. Wang, J.-M. Yan, Y.-F. Zhang, Y. Ping, H.-L. Wang and Q. Jiang, *Nanoscale*, 2014, **6**, 3073–3077.
6 X. Gu, Z.-H. Lu, H.-L. Jiang, T. Akita and Q. Xu, *J. Am. Chem. Soc.*, 2011, **133**, 11822–11825.
7 Z. L. Wang, J. M. Yan, Y. Ping, H. L. Wang, W. T. Zheng and Q. Jiang, *Angew. Chem., Int. Ed.*, 2013, **52**, 4406–4409.
8 M. S. İzgi, Ö. Şahin and C. Saka, *Int. J. Hydrogen Energy*, 2016, **41**, 1600–1608.
9 H. Cai, P. Lu and J. Dong, *Fuel*, 2016, **166**, 297–301.
10 J. Mahmood, S.-M. Jung, S.-J. Kim, J. Park, J.-W. Yoo and J.-B. Baek, *Chem. Mater.*, 2015, **27**, 4860–4864.
11 T. Liu, Q. Wang, B. Yan, M. Zhao, W. Li and H. Bie, *J. Nanomater.*, 2015, **2015**, 1–5.
12 J. Liao, H. Li, X. Zhang, K. Feng and Y. Yao, *Catal. Sci. Technol.*, 2016, **6**, 3893–3899.
13 N.-Z. Shang, C. Feng, S.-T. Gao and C. Wang, *Int. J. Hydrogen Energy*, 2016, **41**, 944–950.
14 J. K. Sun and Q. Xu, *ChemCatChem*, 2015, **7**, 526–531.
15 Q.-L. Zhu, D.-C. Zhong, U. B. Demirci and Q. Xu, *ACS Catal.*, 2014, **4**, 4261–4268.
16 S.-J. Li, Y. Ping, J.-M. Yan, H.-L. Wang, M. Wu and Q. Jiang, *J. Mater. Chem. A*, 2015, **3**, 14535–14538.
17 X. Yang, P. Pachfule, Y. Chen, N. Tsumori and Q. Xu, *Chem. Commun.*, 2016, **52**, 4171–4174.
18 C. Feng, Y. Wang, S. Gao, N. Shang and C. Wang, *Catal. Commun.*, 2016, **78**, 17–21.
19 Q. Lv, L. Feng, C. Hu, C. Liu and W. Xing, *Catal. Sci. Technol.*, 2015, **5**, 2581–2584.
20 L. E. Heim, N. E. Schlörer, J.-H. Choi and M. H. Prechtl, *Nat. Commun.*, 2014, **5**, 1–8.
21 Y. Bi and G. Lu, *Int. J. Hydrogen Energy*, 2008, **33**, 2225–2232.
22 H. Gao, J. Zhang, R. Wang and M. Wang, *Appl. Catal., B*, 2015, **172**, 1–6.
23 Y. Bi, H. Hu, Q. Li and G. Lu, *Int. J. Hydrogen Energy*, 2010, **35**, 7177–7182.
24 X. Pan, L. Wang, F. Ling, Y. Li, D. Han, Q. Pang and L. Jia, *Int. J. Hydrogen Energy*, 2015, **40**, 1752–1759.
25 Y. Li, T. Chen, T. Wang, Y. Zhang, G. Lu and Y. Bi, *Int. J. Hydrogen Energy*, 2014, **39**, 9114–9120.
26 H. Hu, Z. Jiao, J. Ye, G. Lu and Y. Bi, *Nano Energy*, 2014, **8**, 103–109.
27 S. Li, H. Hu and Y. Bi, *J. Mater. Chem. A*, 2016, **4**, 796–800.

 This journal is © The Royal Society of Chemistry 2016

Published on 01 November 2016. Downloaded by University of Newcastle on 07/01/2017 02:00:00.

28 Q.-L. Zhu, N. Tsumori and Q. Xu, *Chem. Sci.*, 2014, **5**, 195–199.
29 Q.-L. Zhu and Q. Xu, *Chemistry*, 2016, **1**, 220–245.
30 G.-G. Park, T.-H. Yang, Y.-G. Yoon, W.-Y. Lee and C.-S. Kim, *Int. J. Hydrogen Energy*, 2003, **28**, 645–650.
31 M.-J. Ledoux and C. Pham-Huu, *Catal. Today*, 2005, **102**, 2–14.
32 H. Zhang, S. Gao, N. Shang, C. Wang and Z. Wang, *RSC Adv.*, 2014, **4**, 31328–31332.
33 R. Feng, M. Li and J. Liu, *Colloids Surf., A*, 2012, **406**, 6–12.
34 T. Sener, E. Kayhan, M. Sevim and Ö. Metin, *J. Power Sources*, 2015, **288**, 36–41.
35 H. A. Miller, M. Bellini, F. Vizza, C. Hasenoehrl and R. Tilley, *Catal. Sci. Technol.*, 2016, **8**, 6870–6878.
36 W. Wang, T. He, X. Liu, W. He, H. Cong, Y. Shen, L. Yan, X. Zhang, J. Zhang and X. Zhou, *ACS Appl. Mater. Interfaces*, 2016, 20839–20848.
37 Q. L. Zhu, N. Tsumori and Q. Xu, *J. Am. Chem. Soc.*, 2015, **137**, 11743–11748.
38 D. Wang and Y. Li, *Adv. Mater.*, 2011, **23**, 1044–1060.
39 A. K. Singh and Q. Xu, *ChemCatChem*, 2013, **5**, 652–676.
40 Y. Huang, X. Zhou, M. Yin, C. Liu and W. Xing, *Chem. Mater.*, 2010, **22**, 5122–5128.
41 X. Zhou, Y. Huang, W. Xing, C. Liu, J. Liao and T. Lu, *Chem. Commun.*, 2008, 3540–3542.
42 S. Kapoor, F. Barnabas, M. Sauer Jr, D. Meisel and C. Jonah, *J. Phys. Chem.*, 1995, **99**, 6857–6863.